Dispersion and Attenuation for the Anelastic Velocity-Memory-Stress System

David F. Aldridge and Leiph A. Preston, Sandia National Laboratories*

Summary

Dispersion and attenuation relations are derived for both the continuous and discrete velocity-memory-stress systems governing 3D anelastic wave propagation in a standard linear solid. Phase speed and attenuation factor curves extracted from these relations enable optimal selection of spatial and temporal gridding intervals to achieve finite-difference algorithm efficiency, while simultaneously minimizing numerical inaccuracy.

Introduction

Seismic wave propagation within an anelastic medium is governed by a set of nine, coupled, integro-differential equations called the *velocity-stress system.* Stress and strain tensor components are related via a temporal convolution integral. However, assumption of the standard linear solid (SLS) rheology enables conversion of these equations to a coupled partial differential system, albeit at the cost of introducing additional dependent variables called memory variables. This partial differential system is referred to as the *velocity-memory-stress* (VMS) system. A recent summary article by Moczo et al. (2007) gives a rigorous development of the VMS system (including a comprehensive list of references) and describes time-domain finite-difference (FD) solution methods.

We have developed a three-dimensional (3D) explicit, time-domain, FD solution of the isotropic anelastic VMS system, using centered FD operators on staggered temporal and spatial grids. Discretization of the VMS differential equations introduces *numerical* dispersion and attenuation which must be distinguished from their intrinsic counterparts associated with the underlying anelastic continuum. Accordingly, we have derived a discrete dispersion/attenuation relation for the 3D VMS difference system, applicable to staggered FD operators with arbitrary temporal and spatial orders. Moreover, the SLS may be represented by an arbitrary number of attenuation mechanisms. The relation applies to either compressional (P) or shear (S) propagation, and reduces to the well-known isotropic elastic expression when the SLS material attenuation vanishes.

Anelastic VMS System

Constitutive equations relating the stress tensor components σ_{ij} to the displacement vector components u_i for a linear, time-invariant, local, and isotropic anelastic medium are

$$\sigma_{ij} = \left(\psi_P - 2\psi_S\right) * \frac{\partial u_k}{\partial x_k}\delta_{ij} + \psi_S * \left(\frac{\partial u_i}{\partial x_j} + \frac{\partial u_j}{\partial x_i}\right), \qquad (1)$$

where the asterisk denotes temporal convolution, δ_{ij} is the Kronecker delta symbol, and repeated subscripts imply summation. The two convolutional kernels ψ_P and ψ_S are called *rate-of-relaxation functions* (SI unit: P/s) and characterize anelastic P and S deformation, respectively. These functions must be causal, may include distributions (i.e., the temporal Dirac delta function $\delta(t)$ and/or its derivatives), and are necessarily minimum-phase.

For an SLS, the rate-of-relaxation functions are a linear combination of the Dirac delta function with a set of one-sided decaying exponentials:

$$\psi_{P,S}(t) = M_{P,S}\left[\delta(t) - \sum_{r=1}^{R} a_{P,S}^r\, \omega^r e^{-\omega^r t} H(t)\right], \qquad (2)$$

where $H(t)$ is the Heaviside unit step function. Each function has *R attenuation mechanisms*, characterized by an amplitude scalar a^r (dimensionless) and a decay rate ω^r (radians/s). Superscript r is merely an index, and should not be interpreted as an exponent. $M_{P,S}$ are the infinite-frequency anelastic moduli:

$$M_P = \lambda + 2\mu, \qquad M_S = \mu,$$

where λ and μ may be termed infinite-frequency Lamé coefficients. In general, all anelastic medium parameters may vary with spatial position **x**.

The anelastic VMS system consists of the 9+6R coupled, first-order, inhomogeneous, partial differential equations

$$\rho\frac{\partial v_i}{\partial t} - \frac{\partial \sigma_{ij}}{\partial x_j} = f_i + \frac{\partial m_{ij}^a}{\partial x_j}, \qquad (3a)$$

$$\frac{\partial r_{ij}^r}{\partial t} + \omega^r r_{ij}^r + \omega^r\left[a_P^r\left(\lambda + 2\mu\right)\frac{\partial v_k}{\partial x_k}\delta_{ij} + a_S^r \mu\left(\frac{\partial v_i}{\partial x_j} + \frac{\partial v_j}{\partial x_i} - 2\frac{\partial v_k}{\partial x_k}\delta_{ij}\right)\right] = 0, \qquad (3b)$$

$(r = 1,2,3,\ldots R)$

$$\frac{\partial \sigma_{ij}}{\partial t} - \lambda \frac{\partial v_k}{\partial x_k}\delta_{ij} - \mu\left(\frac{\partial v_i}{\partial x_j} + \frac{\partial v_j}{\partial x_i}\right) - \sum_{r=1}^{R} r_{ij}^{r} = \frac{\partial m_{ij}^{s}}{\partial t}, \quad (3c)$$

where v_i are velocity vector components, σ_{ij} are stress tensor components, and r^r_{ij} are symmetric memory tensor components (SI unit: P/s). Equations (3a) are Cauchy's linearized equations of motion, representing conservation of mass and linear momentum for a continuum (ρ is mass density). Equations (3c) are time-differentiated constitutive relations obtained by combining (1) and (2), and adopting a suitable definition for the memory variables. As indicated in (3b), these memory variables are coupled to gradients of the velocity vector components. Finally, inhomogeneous terms in the VMS system represent various body sources of seismic waves: $f_i(\mathbf{x},t)$ is the force density vector and $m_{ij}(\mathbf{x},t)$ is the moment density tensor. Note that the moment density tensor is split into symmetric and anti-symmetric parts, indicated by superscripts "s" and "a" respectively.

For FD solution, the dependent variables in (3) are stored on uniformly-spaced, staggered, spatial and temporal grids (Figures 1 and 2). The primary advantage of staggered storage schemes over alternative non-staggered approaches pertains to greater accuracy in numerical differentiation and interpolation. Enhanced accuracy leads, in turn, to reduced numerical dispersion/attenuation in the FD solution. All partial derivatives in (3) are numerically approximated with centered, staggered, FD operators with M-order accuracy in time and N-order accuracy in space (where M and N are even integers). Explicit time-updating formulae for the 9+6R dependent variables are readily derived.

Temporal and spatial FD operator coefficients are designated a_m (m = 1,2,3,…M/2) and b_n (n = 1,2,3,….N/2), respectively. The memory variable updating expression derived from (3b) requires a temporal interpolation scheme. We take the order of this interpolation operator identical to the temporal FD order, and denote the interpolation coefficients as c_m (m = 1,2,3,…M/2).

Continuous Dispersion/Attenuation Relation

We utilize classical von Neumann analysis to derive a dispersion/attenuation relation for the VMS partial differential system (3). First, assume a homogeneous anelastic wholespace without body sources of seismic waves. Next, Fourier transform the VMS system from time t to angular frequency ω, and eliminate stress tensor and memory tensor components. Finally, assume the remaining three velocity vector components are described by a plane wave progressing in the direction of unit vector $\mathbf{n}$:

$$V_i(\mathbf{x},\omega) = V_i(\mathbf{0},\omega)\exp\left[+iK(\omega)(\mathbf{x}\cdot\mathbf{n})\right],$$

where $K(\omega)$ is a *complex wavenumber* to be determined. The result is 3 × 3 system of homogeneous linear algebraic

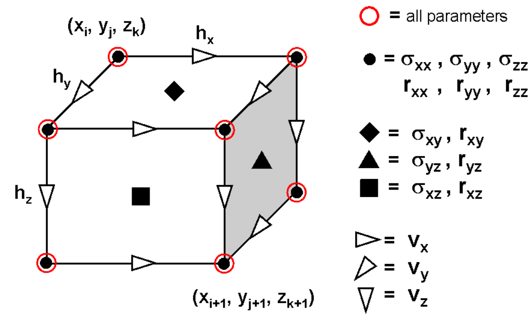

Figure 1. Spatial storage scheme for anelastic wavefield variables and earth model parameters.

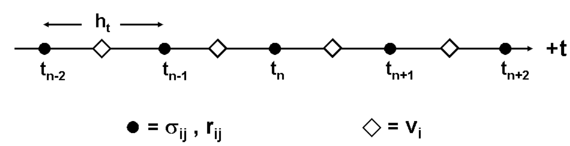

Figure 2. Temporal storage scheme for anelastic wavefield variables.

equations for the (transformed) velocity vector components at the coordinate origin $V_i(\mathbf{0},\omega)$. Nontrivial solutions exist when the determinant of the coefficient matrix vanishes. This yields the dispersion/attenuation relation for the continuous space-time VMS system

$$K(\omega) = \frac{\omega}{c_\infty}\left[1 - \sum_{r=1}^{R}\frac{a^r}{1 - i\left(\omega/\omega^r\right)}\right]^{-1/2}, \quad (4)$$

where c_∞ is the *infinite-frequency* phase speed for either P or S waves:

$$\text{P-waves:} \quad c_\infty = \sqrt{\frac{\lambda + 2\mu}{\rho}}, \qquad \text{S-waves:} \quad c_\infty = \sqrt{\frac{\mu}{\rho}}.$$

The real and imaginary parts of the complex wavenumber are given by $K(\omega) = [\omega/c(\omega)] + i\alpha(\omega)$, where $c(\omega)$ is the *phase speed* and $\alpha(\omega)$ is the *attenuation factor*. After the right side of equation (4) is evaluated over the frequency range of interest, the phase speed and attenuation factor functions are easily obtained via

$$c(\omega) = \frac{\omega}{\mathrm{Re}\{K(\omega)\}}, \qquad \alpha(\omega) = \mathrm{Im}\{K(\omega)\}. \quad (5a,b)$$

We emphasize that the dispersion/attenuation relation (4) applies to either 3D P or S waves, and accommodates an arbitrary number of SLS attenuation mechanisms. Moreover, as expected, both the phase speed and attenuation factor are isotropic (independent of the propagation direction **n**). In the case where all SLS amplitude factors vanish, (4) reduces to the elastic counterpart $K(\omega) = \omega/c$, where the wavenumber is strictly real-valued (α vanishes and c is independent of frequency).

Discrete Dispersion/Attenuation Relation

The dispersion/attenuation relation for the discrete VMS system is obtained by an identical derivational procedure. We apply a discrete-time Fourier transform (Oppenheim and Willsky, 1983) from sampled time t_n to continuous frequency ω to the 9+6R FD updating formulae, yielding

$$\sqrt{K_x^2(\omega) + K_y^2(\omega) + K_z^2(\omega)} = \frac{\Omega(\omega)}{c_\infty}\left[1 - \sum_{r=1}^{R} \frac{a^r}{1 - i\left(\Omega(\omega)/\Omega^r(\omega)\right)}\right]^{-1/2} . \qquad (6)$$

Note the similarity of this expression to the continuous dispersion/attenuation relation (4). Frequency-dependent quantities on the right side depend on the temporal difference and interpolation operators, and are defined as

$$\Omega(\omega) \equiv \frac{2}{h_t}\sum_{m=1}^{M/2} a_m \sin\left[\left(2m-1\right)\frac{\omega h_t}{2}\right],$$

$$\Omega^r(\omega) \equiv 2\omega^r \sum_{m=1}^{M/2} c_m \cos\left[\left(2m-1\right)\frac{\omega h_t}{2}\right].$$

$\Omega(\omega) \to \omega$ and $\Omega^r(\omega) \to \omega^r$ as the FD timestep h_t vanishes. Left side quantities depend on the spatial FD operator via

$$K_x(\omega) \equiv \frac{2}{h_x}\sum_{n=1}^{N/2} b_n \sin\left[\left(2n-1\right)\frac{K(\omega)h_x n_x}{2}\right],$$

and similarly for $K_y(\omega)$ and $K_z(\omega)$. The sine function in this expression has a complex-valued argument, and thus is interpreted as $\sin(z) = [\exp(+iz)\text{-}\exp(-iz)]/2i$ where $z = x+iy$ is a complex number.

In the limit as spatial and temporal discretization intervals vanish, expression (6) approaches the continuous space-time dispersion/attenuation relation (4). Finally, if the SLS amplitude scalars vanish, (6) reduces to the discrete elastic (or acoustic) dispersion relation given by Moczo et al. (2000) and Aldridge and Haney (2008).

Discrete Phase Speed and Attenuation Factor

Extraction of the frequency-dependent phase speed and attenuation factor functions from the discrete dispersion/attenuation relation (6) is complicated by the fact that the complex wavenumber $K(\omega)$ appears within the arguments of the sine functions. Nevertheless, in the special case of a cubic grid ($h_x = h_y = h_z = h$), these can be obtained if plane wave propagation is restricted to one of the three principal directions illustrated in Figure 3.

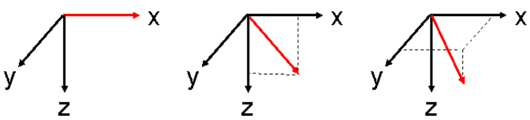

Figure 3. Plane wave propagation directions through a 3D spatial grid. Left: along a coordinate axis. Middle: along a coordinate-plane diagonal. Right: along a body diagonal.

The discrete dispersion/attenuation relation becomes

$$\sum_{n=1}^{N/2} b_n \sin\left[(2n-1)\frac{K(\omega)h_e}{2}\right] = \frac{h_e\Omega(\omega)}{2c_\infty}\left[1 - \sum_{r=1}^{R}\frac{a^r}{1 - i\left(\Omega(\omega)/\Omega^r(\omega)\right)}\right]^{-1/2}, \qquad (7)$$

where h_e is an *effective* spatial grid interval defined by

$$h_e \equiv 1/\sqrt{1}, \qquad 1/\sqrt{2}, \qquad 1/\sqrt{3},$$

according to the three principal directions. Next, the multiple-angle sine functions are expanded in power series (Gradshetyn and Ryzhik, 1993). We obtain

$$\sum_{n=1}^{N/2} B_n \sin^{2n-1}\left[\frac{K(\omega)h_e}{2}\right] - \frac{h_e\Omega(\omega)}{2c_\infty}\left[1 - \sum_{r=1}^{R}\frac{a^r}{1 - i\left(\Omega(\omega)/\Omega^r(\omega)\right)}\right]^{-1/2} = 0, \qquad (8)$$

where the expansion coefficients B_n are linear combinations of the spatial FD operator coefficients b_n. Equation (8) is a polynomial of order N-1 in $\sin(K(\omega)h_e/2)$. All coefficients *except* the constant term are real-valued. Extraction of the approximate ROOT of the polynomial enables the complex wavenumber to be determined via

$$K(\omega) = \frac{2}{h_e}\sin^{-1}\left(\text{ROOT}\right), \qquad (9)$$

where the arcsin function is understood as complex-valued. Discrete-medium phase speed and attenuation factor are then obtained via equations (5a,b).

Anelastic Dispersion and Attenuation

Numerical Example

Figure 4 displays phase speed, attenuation factor, and quality factor as functions of frequency (in Hz) for an SLS with R = 3 attenuation mechanisms. Quality factor is obtained from phase speed and attenuation factor via

$$Q(\omega) = \frac{1}{2}\left[\frac{\omega}{c(\omega)\alpha(\omega)} - \frac{c(\omega)\alpha(\omega)}{\omega}\right].$$

Green/red curves pertain to the continuous/discrete VMS systems. Plane wave propagation is along the $+x$-axis, and FD operator orders are M=2 and N=4 (with conventional Taylor series coefficients). The timestep h_t equals the *elastic* CFL stability limit, but is calculated with the infinite-frequency *anelastic* wavespeed. This particular SLS is optimally designed to yield $Q(f) \approx 100$ over the bandwidth 5-500 Hz, with phase speed c = 2000 m/s at f = 100 Hz (Aldridge, 2000). Clearly, algorithm performance departs from the ideal situation at about $f \sim 200$ Hz.

The same information is re-plotted in Figure 5 with respect to the FD sampling parameter $s = h/\lambda_d = hf/c_d(f)$, where λ_d is a wavelength within the discrete grid. s =0.5 corresponds approximately to f =1000 Hz. Curves are normalized by dividing by the corresponding continuous space-time quantity (subscript "c"), implying the horizontal green line at unity represents ideal algorithm performance. The vertical blue line corresponds to the conventional "5 grid intervals per wavelength" rule of thumb for dispersion-free numerical wave propagation. Although phase speed is indeed within +1/2% of the ideal, the attenuation factor and quality factor deviate by +3.5% and -4%, respectively.

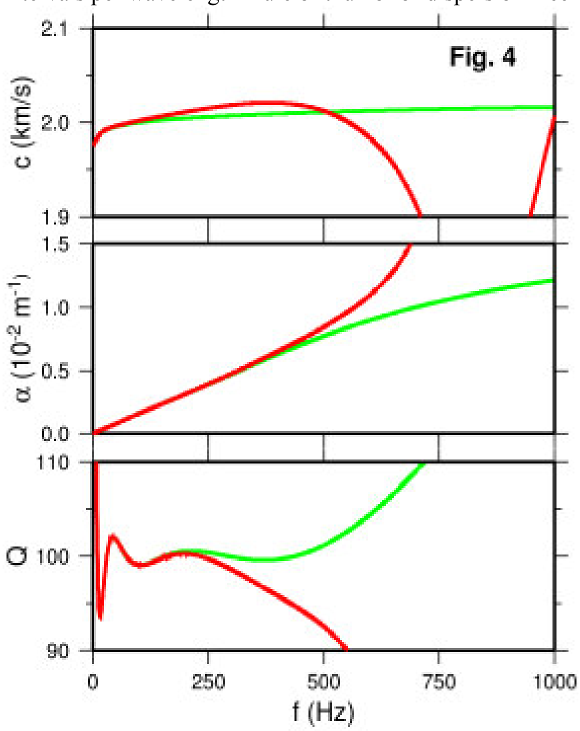

Conclusions and Ongoing Work

We have developed a numerical dispersion/attenuation relation for the 3D isotropic anelastic VMS system, solved via O(M,N) FD operators on staggered spatial and temporal grids. Phase speed and attenuation factor curves extracted from this relation enable optimal selection of spatial and temporal grid intervals to achieve algorithmic efficiency, with minimal numerical dispersion and attenuation. Additional work entails developing a solution methodology addressing arbitrary wave propagation directions, high spatial order FD operators (where extracting roots of a high-order polynomial are required), group speed, and understanding the CFL stability condition for the discrete VMS system. Finally, the derivational methodology applies to other partial differential systems governing wave propagation in attenuative media (e.g., electromagnetic or poroelastic waves).

Acknowledgement

Sandia National Laboratories is a multiprogram science and engineering facility operated by Sandia Corporation, a Lockheed-Martin company, for the US Department of Energy's National Nuclear Security Administration, under contract DE-AC04-94AL850.

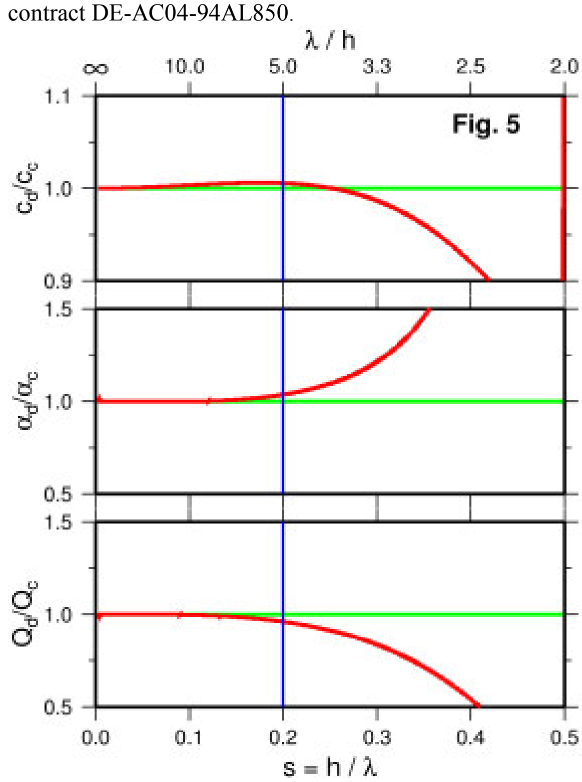

References

Aldridge, D.F., 2000, Seismic Q modeling with the standard linear solid: 70th Annual Meeting and International Exposition, Society of Exploration Geophysicists, Calgary, Alberta, Canada.

Aldridge, D.F. and Haney, M.M., 2008, Numerical dispersion for the conventional-staggered-grid finite-difference elastic wave propagation algorithm: Technical report SAND2008-4991, Sandia National Laboratories.

Gradshteyn, I.S., and Ryzhik, I.M., 1994, Table of integrals, series, and products, fifth edition: Academic Press.

Moczo, P., Kristek, J., and Halada, L., 2000, 3D fourth-order staggered-grid finite-difference schemes: stability and grid dispersion: Bulletin of the Seismological Society of America, **90**, 587-603.

Moczo, P., Robertsson, J.O.A., and Eisner, L., 2007, The finite-difference method for modeling of seismic wave propagation: Advances in Geophysics, **48**, 421-516.

Oppenheim, A.V., and Willsky, A.S., 1983, Signals and systems: Prentice-Hall.